Journal of Pharmaceutical Innovation (2024) 19:24
https://doi.org/10.1007/s12247-024-09834-w

ORIGINAL ARTICLE

Silver Sulfadiazine Nanocrystal-Based Hydrogels: The Impact of Lipid Components on *In-vitro* and *Ex-vivo* Release, Bacterial Biofilm Permeability, and *In-vitro* Antibacterial Activity

Anh Quang Luong[1,2] · Hien Thanh-Thi Pham[3] · Bao Ngoc Tran[3] · Tiep Khac Nguyen[4] · Chien Ngoc Nguyen[3,5]

Accepted: 22 April 2024 / Published online: 9 May 2024

Abstract

Purpose This study developed a new formulation for silver sulfadiazine (SSD) nanocrystal-based hydrogels for in vitro antimicrobial activity.

Methods SSD nanocrystals were prepared by using a wet-mill apparatus; effects of polymers, surfactants and lipid-based carriers were investigated. The gel-forming chemicals were subsequently dispersed in the SSD nanocrystal nanosuspensions, resulting in homogeneous hydrogels. The antibacterial activities of new formulations were tested in-vitro.

Results The final SSD nanocrystal formulation (less than 300 nm, PDI: 0.300) containing glyceryl monostearate (GMS) or lecithin (Lec), combining with hydrophilic polymers (hydroxypropyl methyl cellulose and polyvinyl alcohol). The artificial neural network was utilized to confirm the effects of lipid ingredients in wet-milling process. Hydroxyethyl cellulose was chosen to formulate the hydrogel which formed the white, smooth, homogeneous, and stable hydrogel after 4 weeks at the room condition. The hydrogel also presented higher and more sustained drug release using Franz's diffusion cells as compared with reference marketed drug and control hydrogels. The efficacy of antibacterial activity shown on the biofilm demonstrated effect of particle size, lipid carriers, and probably interaction between SSD with biofilm membrane.

Conclusion These findings implied a potential application of SSD nanocrystal-lipid carrier-based hydrogels in clinical practice.

Keywords Silver Sulfadiazine · Nanocrystals · Hydrogels · Biofilm Permeation · Antimicrobial Activity · Artificial Neural Network

Introduction

Infection is a main issue for wounds due to burn injuries. Wound infection delays the healing process of injuries by prolongating the inflammatory phase of the immune response in human being [1]. Nowadays, there are many therapeutics that have been introduced for treatment of wound infection, and applying antibiotic groups still shows the leading role for the target of controlling bacterium growth. However, silver sulfadiazine (SSD), a chemical complex compounded by sulfadiazine and silver, is widely used as a topical antibacterial treatment in many clinical burn units over the world [2]. The sulfadiazine constituent functions as a sulfonamide antibiotic, which has a broad-spectrum action against both gram-negative and gram-positive bacteria by demolishing the cell membrane and inhibiting DNA replication [3, 4]. The release of free silver ions (from SSD),

✉ Tiep Khac Nguyen
tiepnk@hup.edu.vn

✉ Chien Ngoc Nguyen
chiennn@hup.edu.vn

1 Department of Pharmacy and Medical Equipment, National Burn Hospital, Hanoi, Vietnam

2 Educational Institute of Pharmacy, Vietnam Military Medical University, Hanoi, Vietnam

3 Faculty of Pharmaceutics and Pharmaceutical Technology, Hanoi University of Pharmacy, Hanoi, Vietnam

4 Faculty of Biotechnology, Hanoi University of Pharmacy, 13-15 Le Thanh Tong Street, Hoan Kiem district, Hanoi, Vietnam

5 National Institute of Pharmaceutical Technology, Hanoi University of Pharmacy, 13-15 Le Thanh Tong Street, Hoan Kiem district, Hanoi, Vietnam

hindering bacterial respiration and production, contributed significantly to the antibacterial effects [3, 4].

Unfortunately, the application of SSD is restricted because of its physical properties [5, 6]. Due to the complexation of silver with the weak sulfonic acid, SSD is insoluble in both water (neutral pH) and several popular solvents such as ethanol or ether [7, 8]. Because of its poor solubility in both hydrophilic and hydrophobic fluids, SSD is difficult to permeate biological membranes such as bacterial cell-wall or biofilm [5, 6]. SSD is insoluble in water and ethanol as well as other popular solvents such as acetone and ether, that caused difficulties in the preparation process of the conventional semi-solid dosage form. Actually, commercial products used micro-sized SSD for O/W cream (1% SSD in Silvadene® cream). Therefore, nanoparticles of SSD can be proposed to both facilitate the preparation of topical drugs and improve its anti-bacterial effects.

In case of infection on wound area, efficacy of antibiotic is limited. The antibiotics remain in a short time on (or into) the skin, leading to an inconsistent concentration of antibiotics [4, 9]. Especially, prolonged use of topical medications on the skin can lead to the activation of antibiotic resistance in bacteria. In which resistance emerges through the formation of biofilm, a bio-membrane composed of polysaccharides, polymer complexes, and cell-wall fragments [9]. Bacteria inside these biofilms will be protected from anti-bacterial agents and host defense mechanisms, thereby reducing the therapy effectiveness. Nanoparticle of SSD is hypothesized to penetrate biofilm, to reverse this situation. Thus, reducing particle size of SSD material to nanosized is reasonable to enhance solubility, permeability, particularly biofilm permeability, and pharmacological activities [10]. In fact, Venkataraman or Gao L et al. used a high-pressure homogenization technique for preparing SSD nanosuspensions (367.85 nm), in which SSD (0.5%) nanogel were more effective in burn *in-vivo* model in comparison with the marketed creams [11, 12]. By preparing into lipid-based nanoparticles (50 to 500 nm) of SSD loaded in hydrogels, the % SSD permeation and % accumulation were higher than the commercial cream [13, 14], which implied a less frequency of gel application. While there are publications that suggest the role of nano-sized SSD, none of them have carried out experiments of the biofilm permeability yet.

In this study, SSD nanoparticles prepared by the wet-milling technique were regarded as a practical method in both laboratory and industry [10, 15]. Compared to hot-melt homogenization [14] or micro-precipitation [11], the wet-milling technique can easily apply to SSD, as the substance is insoluble in both organic solvents and water. Furthermore, the wet-milling process is easily scalable due the availability of machine scale, making it suitable for large-scale production [12, 15, 16].

Among the preparations to be applied on damaged skin (e.g. burn wound, chronic wound…), gels have shown its preeminent as it can provide a moist environment for the wound and release the drug to the wound bed concurrently [12]. In addition, the gel materials support to constitute a water-soluble film on damaged skin after drying, which supplies prolonged antimicrobial activity and are removed easily whilst the bandage changes are executed. Therefore, we developed an SSD nanocrystal loaded lipid carrier - hydrogel using wet milling technique, in which the role of lipid ingredient was illustrated. Also, the therapeutic effects on bacterial biofilm and *in-vitro* antibacterial activities of the obtained nanoparticle-loaded hydrogels were evaluated in this work.

Materials and Methods

Chemicals and Reagents

SSD was obtained from Indian Phosphate Limited (Ujain, India). Hydroxypropyl methyl cellulose E6 (HPMC E6), polyvinyl alcohol (PVA), and hydroxyethyl cellulose (HEC) were purchased from Zhejiang Zhongbao Co. (Beijing, China). Sodium carboxymethyl cellulose (CMC) was purchased from Daicel Corporation (Tokyo, Japan). Carbopol® 940 (Cbp940) was obtained from Lubrizol Corporation (USA). Tween 80 was obtained from Xilong Scientific Co., Ltd. (Shanghai, China); Sodium lauryl sulfate (SLS) was purchased from Merck & co. (Darmstadt, Germany). Sodium docusate (SD) was procured from Sigma-Aldrich Pte., Ltd. (Darmstadt, Germany). Poloxamer 407 was purchased from BASF (Darmstadt, Germany). Precirol ATO5 was obtained from Gattefosse S.A. (France). Lecithin was procured from Kanto Chemical Co. (Kanto, Japan). Glyceryl monostearate (GMS) was obtained from Thai Duong (Ha Nam, Viet Nam). Phosphoric acid, ammonia, and HPLC-grade acetonitrile were purchased from Merck Co. (Darmstadt, Germany). All other reagents and solvents were of analytical grade and used without further purification. Silvirin® cream containing 1% SSD as a reference marketed drug was obtained from Raptakos Brett Co., Ltd. (India).

Animals and Bacteria

Male Sprague-Dawley rat skins were supplied from Military Medical University (Hanoi, Vietnam) for in vitro and ex vivo studies. The bacterial *Staphylococcus aureus* ATCC 33,591, (Gram +) and *Escherichia coli* ATCC 25,922 (Gram -) were used as tested microorganisms.

Preparation of SSD Nanocrystal Formulations, Hydrogels and Controls

Prepare SSD nanocrystal suspension:

SSD nanocrystals were prepared by a wet milling method (Fig. 1); different compositions of ingredients were listed in Table 1. Solid and liquid lipids (Table 1) were melted at 70 °C in a glass beaker, then SSD was subsequently dispersed in the lipid mixture to generate a uniform mixture (the lipid phase). Other ingredients (polymers, stabilizers, and surfactants) were dissolved in water (the water phase). Finally, all liquid and aqueous phases were placed into milling chambers (Tencan XQM-2 A, Hunan, China). The milling process was set up with the following parameters: Speeds of 500 rpm, continuous operating times with 10 min of interval after each 1 h running, the size of the zirconia milling balls (300 g) of 5.0 mm. The SSD nanocrystal suspensions were obtained through ball milling progressing for periods ranging from 2 to 5 h.

Prepare SSD nanoparticle hydrogel:

SSD Nanoparticle Hydrogel Afterwards, gel-forming agents (HEC, or CMC, or Cbp940, mentioned in Table 2) were dispersed into formed SSD nanosuspensions (1000 rpm, magnetic stirring). The hydrogels were prepared at a scale of 10 g (equivalent to 1% SSD, w/w).

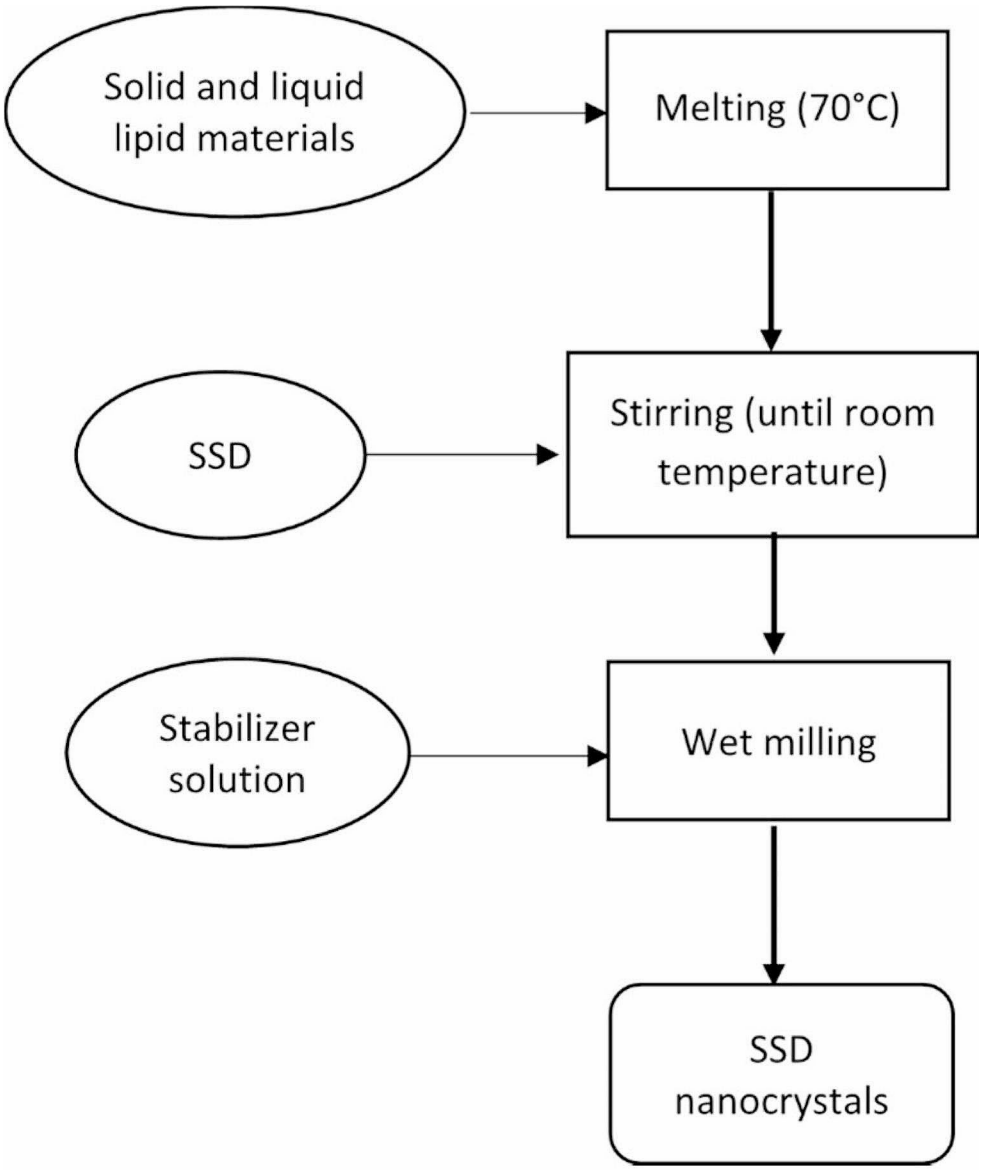

Fig. 1 Illustration of SSD nanocrystal preparation

Table 1 Composition of different SSD nanocrystal formulations

Formulations	SSD (%)	HPMC E6 (%)	PVA (%)	Tween 80 (%)	SLS (%)	SD (%)	Poloxamer 407 (%)	GMS (%)	Precirol ATO5 (%)	Lecithin (%)	Variable types
F1	2	1	0.5	-	-	-	-	-	-	-	HPMC: PVA ratios
F2	2	1	1	-	-	-	-	-	-	-	
F3	2	0.5	1	-	-	-	-	-	-	-	
F4	2	0.5	0.5	-	-	-	-	-	-	-	
F5	2	0.5	1	0.25	-	-	-	-	-	-	Surfactant types
F6	2	0.5	1	-	0.25	-	-	-	-	-	
F7	2	0.5	1	-	-	0.25	-	-	-	-	
F8	2	0.5	1	-	-	-	0.25	-	-	-	
F9	2	0.5	1	-	0.1	-	-	-	-	-	SLS concentrations
F10	2	0.5	1	-	0.2	-	-	-	-	-	
F11	2	0.5	1	-	0.35	-	-	-	-	-	
F12	2	0.5	1	-	-	-	-	1	-	0.5	Lipid types
F13	2	0.5	1	-	-	-	-	2	-	0.5	
F14	2	0.5	1	-	-	-	-	-	1	0.5	
F15	2	0.5	1	-	-	-	-	-	2	0.5	
F16	2	0.5	1	-	-	-	-	3	-	0.5	GMS concentrations
F17	2	0.5	1	-	-	-	-	4	-	0.5	
F18	2	0.5	1	-	-	-	-	5	-	0.5	
F19	2	0.5	1	-	-	-	-	3	-	0.1	Lecithin concentrations
F20	2	0.5	1	-	-	-	-	3	-	0.25	
F21	2	0.5	1	-	-	-	-	3	-	0.75	
F22	3	0.5	1	-	-	-	-	3	-	0.5	SSD concentrations
F23	4	0.5	1	-	-	-	-	3	-	0.5	
F24	5	0.5	1	-	-	-	-	3	-	0.5	
F25	6	0.5	1	-	-	-	-	3	-	0.5	

SSD raw suspension: SSD raw material (D90: 133 μm, span 2.419 μm, measured by Mastersizer Micro, Malvern Panalytical., Cambridge, United Kingdom) was dispersed in water together with the same ingredients using ceramic pestle and mortar. The formed micro suspensions were used as a control to compare with the SSD nanosuspension (prepared by the wet-milling process).

SSD Solution Hydrogel SSD raw material was dissolved in 28% aqueous ammonia (equivalent to 1% SSD, *w/w*). Then chosen gelling agent was dispersed into the above SSD solution; formed hydrogels were used as a control to compare with the SSD nanosuspension (prepared by the wet-milling process).

Characterization of SSD Nanocrystals and Hydrogels

Measure Average Particle Size (Dynamic Light Scattering)

The average particle size, polydispersity index (PDI) of SSD nanocrystals were measured at 25 ± 2 °C by using Zetasizer Ultra Nano ZS90, Malvern, UK. All prepared samples were diluted 10 times with water; each measurement was performed in triplicate with a count rate in the range of 200–400 kcps.

Assay Drug Content

SSD concentrations were determined by high performance liquid chromatography (HPLC, Agilent Technologies 1260 Infinity, Agilent Technologies, Santa Clara, CA, USA). The HPLC column used was Inert Sustain C18 (250 × 4.6 mm; 5 μm). HPLC conditions were 1.2 mL/min flow-rate, 10 μL injection volume; the mobile phase was a mixture of 99:1:900 (v/v/v) acetonitrile, phosphoric acid, and water.

Short-term stability test via centrifugation:

As SSD was insoluble in the carrier, the short-term stability of SSD suspensions are tested. The mild centrifugation (1000 rpm, 5 min) was conducted to test the stability of the formed nanosuspension. After centrifugation, the concentration of drug in the supernatant was assayed to compare with the total SSD amount in the nanosuspension. The %drug centrifugation was calculated as:

$$\%drug\,(centrifugation) = \frac{Concentration\ of\ SSD\ in\ supernatant}{Total\ SSD\ in\ nanosuspension} \times 100\,(\%)$$

Table 2 Particle size, PDI, and SSD content after centrifugation of different SSD nanocrystal formulations (mean ± SD, $n = 3$)

Formulation	Size	PDI	Short-term stability (*) % SSD content
F1	318 ± 5	0.171 ± 0.014	47.24
F2	313 ± 6	0.169 ± 0.035	48.19
F3	304 ± 4	0.209 ± 0.028	56.92
F4	326 ± 4	0.178 ± 0.026	41.06
F5	294 ± 12	0.242 ± 0.024	35.15
F6	248 ± 6	0.288 ± 0.006	45.33
F7	289 ± 7	0.192 ± 0.008	40.70
F8	290 ± 2	0.251 ± 0.010	39.62
F9	267 ± 6	0.274 ± 0.033	41.42
F10	269 ± 9	0.268 ± 0.025	44.88
F11	253 ± 8	0.259 ± 0.024	41.26
F12	288 ± 4	0.249 ± 0.024	49.83
F13	278 ± 6	0.156 ± 0.036	65.23
F14	307 ± 2	0.245 ± 0.060	43.07
F15	286 ± 11	0.299 ± 0.081	42.99
F16	**272 ± 5**	**0.219 ± 0.026**	**66.47**
F17	264 ± 8	0.253 ± 0.029	71.28
F18	**285 ± 3**	**0.219 ± 0.015**	**79.95**
F19	305 ± 8	0.262 ± 0.065	51.87
F20	300 ± 6	0.244 ± 0.023	60.27
F21	309 ± 10	0.222 ± 0.058	65.68
F22	290 ± 2	0.215 ± 0.010	58.74
F23	293 ± 1	0.231 ± 0.061	59.23
F24	293 ± 1	0.199 ± 0.058	60.82
F25	297 ± 5	0.217 ± 0.031	59.93

(*)short-term study, %SSD remained in the supernatant after centrifugation at 1000 rpm for 10 min.

Fourier-Transform Infrared Spectroscopy (FT-IR)

FT-IR spectra were measured by Jasco FT-IR 6700 spectrophotometer (Jasco International Co., Ltd., Japan) over the region of 4000–400 cm^{-1}. To obtain the dry powder, SSD nanocrystals or the hydrogel of SSD nanosuspension were freeze-dried at a pressure of 0.1 mbar and a temperature of -40 °C in 24 h using Alpha 1–2 LDplus (Martin Christ GmnH, Harz, Germany). Subsequently, the sample was separately mixed with KBr at a ratio of 1:20 (analyte, w/w). The obtained mixture was compressed into thin plate before measuring.

Differential Scanning Calorimetry (DSC) and X-ray Powder Diffraction (XRPD) Analyses

The DSC analysis was performed using Mettler Toledo DSC 1 (Mettler Toledo, Switzerland). Samples (3–8 mg) were placed in sealed aluminium pans. The heating rate of 10°C/min was used in the temperature range from 0°C to 350°C with a nitrogen air rate of 50 mL/min.

The XRPD analysis was performed for SSD raw material, PMs, and freeze-dried SSD nanocrystal using a D8 Advance diffractometer (Bruker, Germany) with Cu Kα radiation (λ = 1.5406) between 5° and 50° (2θ) at room temperature (25 ± 2 °C).

Visual Appearance and pH

Visual appearance of SSD nanocrystal-based hydrogels was observed for transparency and uniformity. The pH of hydrogels was determined by measuring the 10-time-in-water diluted solution gel (pH meter, Mettler Toledo, Switzerland).

Stability of SSD Nanocrystals and Hydrogels

The stability of SSD nanocrystals was assessed through determining particle size and PDI, SSD content in the hydrogel, visual appearance, and pH of the hydrogel of the samples after 1 week to 4 weeks storage under different conditions: (i) 2 to 8 °C, (ii) 30 °C − 75% RH, and (iii) 40 °C, 75% RH.

Scanning Electron Microscopy (SEM) Characterization

The surface morphology of SSD nanocrystal-based hydrogels was determined using Hitachi S4800 (Hitachi Co., Kyoto, Japan). Samples were placed on a stub and sputter-coated with a thin platinum layer (Ion sputter E-1045; Hitachi) before field emission SEM analysis.

In vitro Drug Release

To perform in vitro drug release studies from SSD nanocrystal-based hydrogels, reference, and controls, membrane diffusion method was adopted using Franz's diffusion cells in Hanson Research system with magnetic stirrers at 32 ± 0.5 °C and 400 rpm (Hanson Research Corporation, USA). Cellulose acetate (CA) membranes were firstly soaked in phosphate buffer (pH 7.4) prepared for 6 receptor compartments and placed between receptor and donor compartment before transferring hydrogel samples. Secondly, 0.3 g hydrogels were transferred into each donor compartment. Then, 1 mL of sample was withdrawn from receptor compartments at time interval of 1, 2, 3, 4, 6, 8, 10, 24 h respectively, and immediately replaced with fresh buffer medium. Finally, the sample was filtered through a 0.45-µm membrane before assaying.

Ex-vivo Skin Permeation Study

This experiment was conducted via dorsal skin of Sprague-Dawley rats. A six-cell Hanson Research diffusion system

(Teledyne Hanson Research, USA; a diffusion area of 1.767 cm^2 and a receptor volume of 7.0 mL) was used. The receiver part was maintained at 32 °C filled with phosphate buffer (pH 7.4). An amount of 0.3 g of SSD nanocrystal-based hydrogel or controls were placed onto the donor part. At the specific time points (0, 1, 2, 3, 4, 6, 8, 10 and 24 h), a 1-mL sample was withdrawn from the receptor, and immediately replaced with fresh buffer medium; the collected sample was then filtered through a 0.45-µm membrane before assaying.

Skin Retention Study

After the completion of the in vitro skin permeation study, rat skin was collected and washed with excess phosphate buffer (pH 7.4). The retained SSD in the skin was extracted by using 2.8% ammonia solution, which was then diluted up 10 times with the mobile phase before HPLC as saying.

In vitro Antimicrobial Activity Assay

The fresh culture of each of the two bacteria, which was suspended in sterile phosphate buffer saline (PBS) to an optical density of 10^8 bacteria/mL, was inoculated on Mueller Hinton agar plates. The original suspension was diluted 100 times with Muller Hinton Broth medium (MHB, CA-MHB, Sigma-Aldrich, St. Louis, MI, USA) to get the working bacterial suspensions (10^6 bacteria/mL).

Measure the Zones of Growth Inhibition

Measurement of the zones of growth inhibition of experimental samples was evaluated by the plate diffusion method on Muller-Hinton agar. HEC gel formulation without SSD was used as controls.

All SSD samples were diluted to 512 µg/mL and 256 µg/mL using PBS medium before adding to each well. Subsequently, 50 µL of the working bacterial suspension was pipetted into each well. Then the 96-well was placed in the incubator (37 °C) for 24 h. Each assay was performed in triplicate. The results were recorded by measuring the zones of growth inhibition surrounding the wells using a Panme calliper (Mitutoyo, Japan) with an accuracy of 0.1 mm.

Determination of Minimum Inhibitory Concentration (MIC)

MICs were measured using Broth microdilution method on 96-well plate (Science Prolab, SPL, Miramar FL, USA). Briefly, the experimental samples were diluted in water to achieve a range of concentrations of 128, 64, 32, 16, 8, 4, 2, 1, 0.5, and 0.025 mg/L, respectively. Then diluted solutions of all samples were added separately to the setting wells. Then, a volume of 100 µL working bacterial suspension was pipetted into each well. The plates were incubated at 37 °C for 24 h. Each assay was performed in triplicate. The MIC values was assessed visually by comparing the culture turbidity.

Biofilm Study

Biofilms (*Staphylococcus aureus)* were grown in 96-well plates at the inoculum of 0.005, OD 620 nm, in Tryptic Soy Broth (TSB) supplemented with 1% glucose and 2% sodium chloride for 24 h at 37 °C.

Then, the biofilm samples were treated with different SSD samples at different concentrations (32, 64, 128, 256, 512, and 1024 µg/mL) for 24 h at 37 °C. The treated biofilm samples were gently washed and sonicated for 5 min to release bacteria from biofilm matrix. Bacterial aliquot(s) were spread on TSB to count colony-forming unit (CFU) after 24 h incubation. The effect of different samples were shown based on CFU. Effects of samples were presented in form of Log (CFU/mL), in which, the control sample was the biofilm sample without SSD treatment [17].

Data Analysis

All results were presented as averages and standard deviation (SD) calculated by SPSS 2016 software (IBM Corporation, NY, USA). The analysis of all data was conducted using JMP 17 Pro (JMP Statistical Discovery LLC, Cary, NC, USA).

Results and Discussion

Preparation and Characterization of SSD Nanocrystal Formulation

Preparation of SSD Nanocrystals

As the wet milling process prepares nanocrystals at a high surface energy, the formed suspension was at a high risk of agglomeration and instability [10]. Different surfactants and polymers were investigated for nanoparticle stabilizers.

Polymeric HPMC E6 and PVA were selected for wet-milling preparations (Table 1). From F1 to F4, different ratios of two polymers were investigated (from 0.5 to 1%). Among them, F3 exhibited the smallest particle size and a higher % SSD in short-term stability (Table 3). Hence, the HPMC: PVA ratio of 1:2 (w/w) was fixed in all formulations. In this case, both HPMC and PVA are steric stabilizer [10, 18], which provide a static barrier for formed nanocrystals. However, polymeric stabilizers are related to such

Table 3 Effect summary of formulation factors on responses (JPM 17 Pro)

	Effect summary		
Source	Factor type	Logworth	*P* value
GMS	Continuous	2.339	0.00459
Variable type(s)	Categorical	1.451	0.03537
Lecithin	Continuous	1.345	0.04517
PVA	Continuous	1.245	0.05686
HPMC E6	Continuous	1.088	0.08166
Precirol ATO	Continuous	0.958	0.11021
Surfactant type(s)	Categorical	0.677	0.21050
SLS(0,0.5)	Continuous	0.565	0.27256
SSD(2,6)	Continuous	0.209	0.61835
Root mean squared error (RMSE)			
Particle size	Response	0.93	0.0061
PDI	Response	0.85	0.0757
%SSD	Response	0.96	0.0004
Overal	Response		

a high viscosity, that reduces milling efficiency. Normally, surfactants should be added into the milling processes.

The effects of non-ionic and ionic surfactants were investigated (F5: Tween 80, F6: SLS, F7: SD, and F8: Poloxamer 407). The F6 product (prepared with SLS) exhibited the best results (particle size of 248 nm, PDI of 0.288, and highest % SSD content (short-term stability) after centrifugation (45.33%). In nanosuspensions, SLS raises nanoparticle stabilization through increasing electrostatic repulsion among nanoparticles [19]. The driving force is formed when the charged surfactant molecules were absorbed onto the crystal surface, which facilitates quick diffusion, intense absorption, and sustained time for desorption of polymer [18]. However, when adding surfactants, the %SSD contents in short-term stability of these formulations were considerably lower than that of F1-F2-F3. As a result, a different approach should be considered.

Effect of Lipid in Preparing SSD Nanocrystals

Aiming for topical application, lipid ingredients were hypothesized to not-only increase the physicochemical stability of the nanosuspensions, but-also modify the bioavailability of dosage forms [20]. Liquid lipid (soybean lecithin) and solid lipids (GMS and Precirol ATO5) were used (F12 to F15, Table 1).

For short-term study, F13 formulation, in which solid lipid (2% GMS) combining with liquid lipid (0.5% Lecithin) increased % SSD content (65%) after centrifugation along with low particle size and PDI (Table 3). Then, increasing solid GMS (3, 4, and 5%, F17-F18, Tables 1 and 3) did increase the %SSD in short-term study. About particle size, relatively small particle sizes (300 nm) were maintained. Finally, with the highest %SSD, F18 was selected for further studies.

It is important to note that this short-term study is not to determine encapsulation efficiency. This test is used for quickly evaluating the physical stability of nanosuspensions, %SSD in short-term stability test shown here reflects sedimentation speed of SSD nanoparticles in suspension. In which, the force from mild centrifugation (1000 rpm, 5 min) induces the faster sedimentation of nanoparticles or nanocrystals than without the nanosuspension without centrifugation. The smaller the particle size, the slower sedimentation, and the longer the physical stability of nanosuspensions. Therefore, higher %SSD implies a better physical stability in this test.

Data Analysis in Preparing SSD Nanocrystals by Artificial Neural Networks

Previously, different suspension formulations (F1 to F25) containing SSD were prepared. However, the experiment design was based on experience, in which the 25 formulations were categorized into 7 groups (column "Variables" in Table 1). By exploiting the capabilities of neural networks, we utilized JMP® (version 17) to derive coefficient values to ascertain the presence of statistically significant factors. This section is only as a screening tool, from which the functions of various ingredients were illustrated. Particularly, the assessment of input effects on outputs were prevented from the human biases during experiments.

Table 4 shows significant variation between these experiments, while a low standard deviation within the repeated measurements was observed. In which, higher Logworth and lower P-value implied a higher significance of the factors. Interestingly, we can show that the critical factors in

Table 4 Particle size and PDI of F18 over 1 week to 4 weeks under different conditions

Time	Storage conditions					
	2-8°C		30°C (75% RH)		40 °C (75% RH)	
	Particle size	PDI	Particle size	PDI	Particle size	PDI
After 1 week	310 ± 2	0.247 ± 0.028	334 ± 6	0.309 ± 0.029	381 ± 10	0.384 ± 0.058
After 2 weeks	299 ± 4	0.242 ± 0.010	324 ± 1	0.283 ± 0.024	373 ± 6	0.352 ± 0.023
After 3 weeks	324 ± 7	0.302 ± 0.043	335 ± 2	0.320 ± 0.008	405 ± 1	0.338 ± 0.033
After 4 weeks	308 ± 2	0.316 ± 0.037	344 ± 12	0.342 ± 0.025	439 ± 7	0.441 ± 0.050

this SSD suspension preparation belong to GMS, Lecithin, and variable types. The "variable type" is a self-defined definition that reflects Table 1. We began experiments using a "base formulation" of HPMC and PVA, referred to previous publications [12, 21]. Based on results, we added several surfactant and lipid components. The high effect of "variable type" is somehow confirming the validity and role of experience in pharmaceutical studies.

Previously, wet milling was often conducted by adding both polymeric stabilizers and surfactants (usually, ionic ones) to increase its efficiency. What a novelty here is that the data suggested to use higher hydrophobic lipids for specific SSD. In fact, the effects of "surfactant types" or SLS concentrations were relatively low compared to lipid ingredients and polymeric ingredients (HPMC or PVA).

Based on the Root Mean Squared Error, the highly valid values of R^2 and p-values confirmed the predicted model and the actual values for particle size and %SSD (short-term study). Therefore Fig. 2, effects of different ingredients were shown. In brief, SSD concentrations from 2 to 6%, or surfactants and SLS concentrations did not affect all the outcomes. Surfactants and SLS concentrations might reduce the particle size as discussed before, but surfactant and SLS might not affect the %SSD. On the other hand, HPMC and PVA (polymeric stabilizers) played as a stabilizer, which lower PDI values (due to the high viscosity, adding HPMC or PVA can improve the monodispersed range of the size, but lower milling efficiency might increase the particle size).

Last, but not least, while particle size was not impacted by GMS and lecithin, these lipid substances did improve %SSD (shown in Fig. 2). Actually, GMS stabilizes polar and nonpolar substances; these qualities of GMS also make it helpful as a dispersant for forming a reservoir as emulsions for SSD (a substance is insoluble in both alcohol and water) [14, 20, 22]. In addition, the mixture of GMS and lecithin facilitated the nanoparticles containing SSD with GMS to make it more stable (as a result, a higher %SSD after centrifugation).

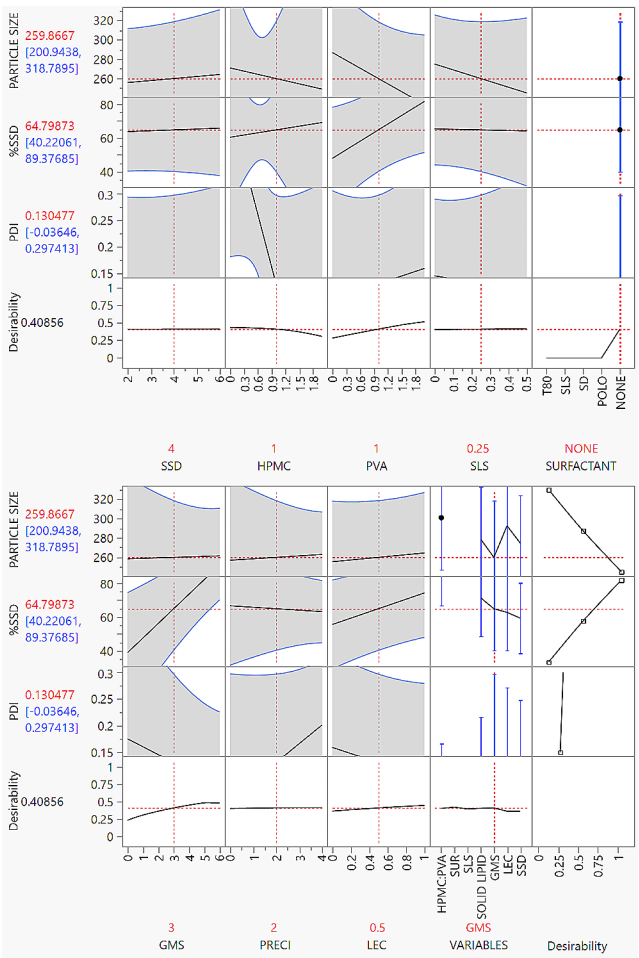

Fig. 2 Effects of formulation factors on 3 responses (particle size, %SSD, and PDI)

Stability Study of the Optimal SSD Nanocrystal Formulation

As selected as the final formulation, F18 was conducted triplicate ($n=3$), particle size was 286.3 ± 23.8 nm, PDI: 0.285 ± 0.064; this result (the average value of three batches) was consistent with F18 in the Table 3 (screening experiment). Size distribution(s) by intensity (measured by Zetasizer Ultra Nano ZS90, Malvern, UK) were presented in Fig. 3D. Then, 3 different samples were mixed, then divided into samples for stability study.

The formulation appearance was unchanged (maintaining a homogenous liquid, without aggregation or flocculation) after 4 weeks. Regarding particle size and PDI (as shown in Table 5), when formulations displayed a rising tendency, using a 2–8 °C refrigerator is the optimal condition. Enduring ambient and accelerated temperatures (30–40 °C with 75% RH), the particle size and PDI were increased at a higher rate. From this result, it suggested that F18 should be in storage condition from 2 to 8 °C to ensure its physicochemical properties and stability.

Physical States and Chemical Interactions of SSD in Nanosuspension

As the Fig. 3A, XRD of the SSD sample (black line) has two strong peaks (8.8° and 10.2°), which was reported before [23]. In the freeze-dried SSD nanocrystal F18 (red line), the intensity values of two peaks are less than that of PM. This result showed that the physical states of SSD nanoparticles were in both the amorphous state and the crystalline state, which is also a specific characteristic of wet-milling technique [15, 16, 21].

Figure 3B shows the DSC curve of SSD raw material (black line) shows two peaks: Endothermic (261 °C) and

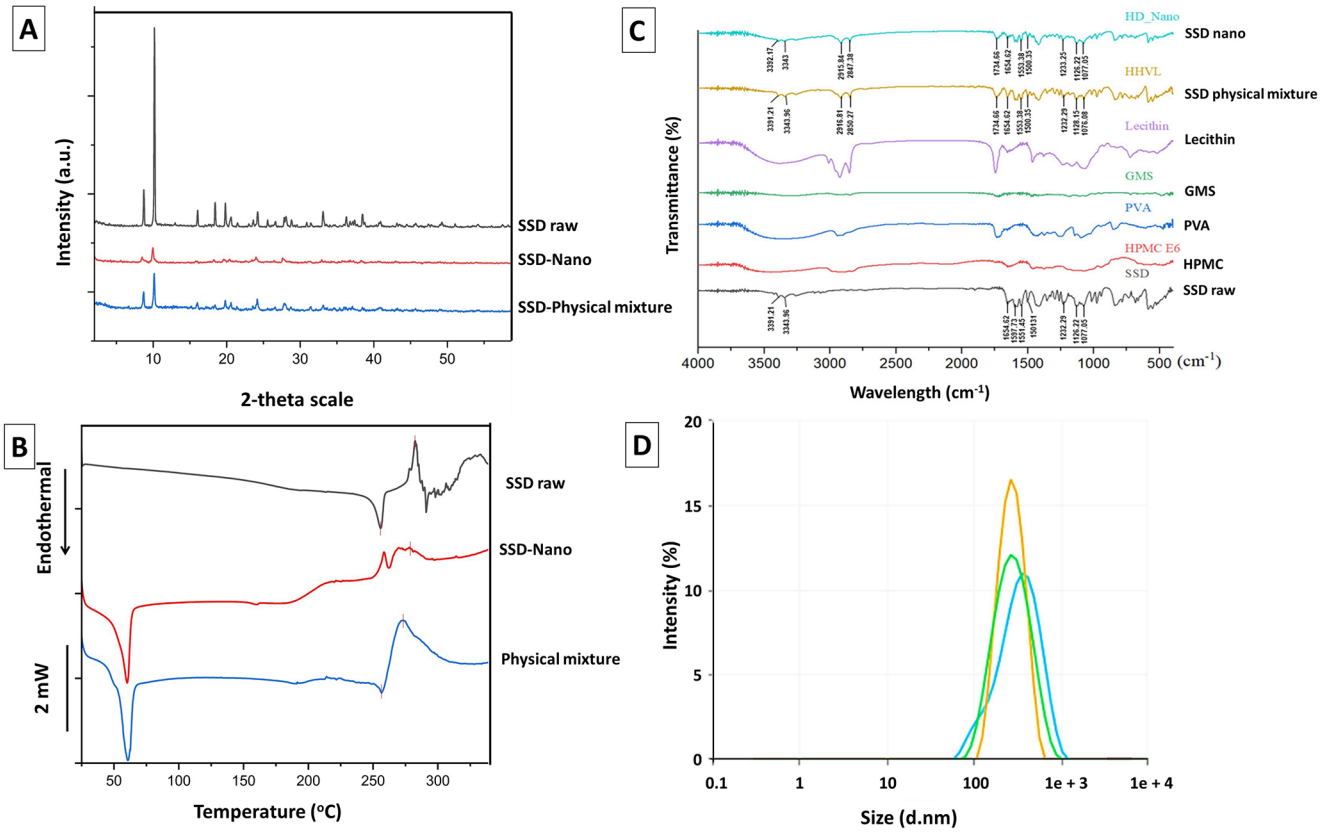

Fig. 3 (**A**) DSC thermograms of SSD raw material, PMs, and freeze-dried SSD nanocrystal; (**B**) XRPD spectrum of SSD raw material, PMs, and freeze-dried SSD nanocrystal; (**C**) FT-IR spectra of SSD raw material, HPMC E6, PVA, GMS, Lecithin, PMs, and freeze-dried SSD nanocrystal; (**D**) Particle size of F18 triplicate batches [* Notes on the Fig: SSD raw (SSD raw material), SSD-Nano (freeze-dried SSD nanocrystal (F18), SSD-Physical mixture (PMs)]

exothermic (280 °C). The endothermic peak attributed to the melting point, while the exothermic peak is attributed to decomposition of the prepared reagent; this finding is complied with reported before [6]. In the PMs (blue line), there are also two endothermal and exothermal peaks of SSD at 261 and 280 °C. Herein, a large endothermal peak is attributed to the melting point of GMS (58 °C). However, melted GMS (at lower temperature) dissolved SSG into liquid state, that is the reason why the endothermal peak of SSD (in Physical mixture, blue line) had a lower intensity. Interestingly, when preparing in form of nanoparticles, the endothermal peak of SSD in the red line was not detected. The result implied that SSD-nano system had a uniformity dispersion of SSD in GMS than physical mixture.

Chemical interactions among components in F18 were characterized by FT-IR spectra (Fig. 3C). SSD raw material produced characteristic absorption peaks at wavelengths of 3391 cm^{-1} and 3343 cm^{-1} (N-H bond), 1232 cm^{-1} and 1126 cm^{-1} (S = O bond), which is similar to the previous report [23]. The characteristic absorption bands of GMS were at 2918 cm^{-1} and 2855 cm^{-1} (C-H bond), 1735 cm^{-1} (C = O bond). The FT-IR spectra of physical mixture (PMs) and freeze-dried SSD nanocrystal F18 showed characteristic absorption peaks of SSD and GMS by cause of the large amount of the two ingredients. The analysis of FT-IR spectra described no interactions between SSD with other excipients used in the preparation.

Preparation and Characterization of SSD Nanocrystal-based Hydrogel

Selection of Gelling Excipients

Gel-forming excipients were selected based on their viscosity at different contents for preparing SSD nanocrystal-based hydrogel including HEC (0.5%, 1%, 1.5%), Cpb940 (0.2%, 0.3%, 0.4%), and CMC (0.5%, 1%, 1.5%) [24]. At the initial time (t = 0), the formulation G3, G4, G5, G6, and G9 showed smooth, and homogeneous states with pH values in the range of 6.0 to 8.0. Based on visual appearance of the 3 formulations in the two accelerated conditions (after centrifugation at 5000 rpm in 15 min, and after storage at 40 °C in 1 week), G3 (HEC 1.5%), G4 (Cbp940 0.2%), and G9 (CMC 1.5%) were chosen for further evaluations (Table 2).

Table 5 Composition and characterizations (visual appearance, pH) of different SSD nanocrystal-based hydrogels

Formulations	Gelling excipient (%)	Visual appearance			pH
		Initial time	After centrifugation at 5000 rpm in 15 min	After storage at 40°C in 1 week	
G1	HEC (0.5)	+	+	+	6.27
G2	HEC (1.0)	++	++	++	6.14
G3	HEC (1.5)	+++	+++	+++	6.34
G4	Cbp940 (0.2)	+++	+++	+++	7.64
G5	Cbp940 (0.3)	+++	+++	+++	7.23
G6	Cbp940 (0.4)	++++	++++	++++	7.41
G7	CMC (0.5)	+	+	+	6.28
G8	CMC (1.0)	+	+	+	6.45
G9	CMC (1.5)	++	++	++	6.51

+, ++, +++, ++++ Different levels of completed visual appearance (lower to higher)

In vitro drug release profiles of SSD nanocrystal-based hydrogels (G3, G4, and G9) were depicted in Fig. 4A. After 24 h, G3 showed the highest release extent (around 80%), whilst G9 and G4 released 77% and 52% of SSD, respectively. As seen in Fig. 4A, the drug release profiles of 3 formulations were characterized by 2 phases: time-dependent phase at early time points (over 50% drug release), followed by a sustained release phase at latter time points. In the sustained release phase, drug release was at the plateau stage. G3 and G9 reached the plateau state after 10 h, meanwhile, G4 presented the saturated SSD release at 4 h. From the above results, G3 (HEC 1.5%) was the chosen SSD nanocrystal-based hydrogel in this study.

Drug Release of Hydrogels and Reference

The effect of SSD nanoparticles was investigated, in which, the permeation study of HEC gels with different SSD preparations: G12 (F4 in HEC, without lipid ingredients), G3 (F18 nanoparticles with lipid ingredients), G10 (SSD prepared in ammoniac solution), and G11 (SSD raw suspension). A commercial marketed drug was conducted as reference for the test.

Figure 4B shows that the % SSD released (after 10 h and 24 h) were in the following order: G10 > G3 (F18) > G12 (F4) > G11 > R. The extremely low SSD release result of reference (9%) could be explained by the fact that topical cream encountered remarkable challenges for liberating SSD out of the excipient matrix including hydrophobic and hydrophilic ingredients when using Franz's diffusion cells. Clearly, the solubility of SSD itself (insoluble in both water and alcohol) caused the drug to impermeable (or incompatible) with cellulose acetate membranes.

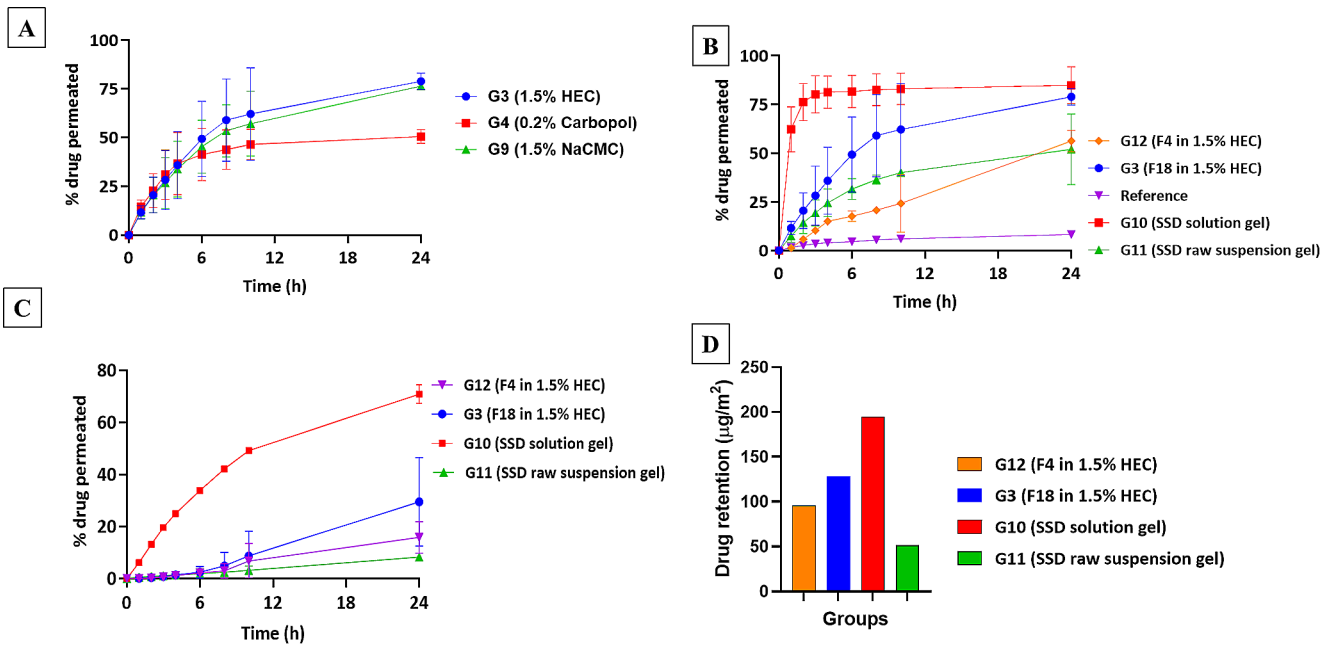

Fig. 4 Effects of lipid ingredients on drug permeability study: (**A**) select gelling agents; (**B**) permeability profiles via cellulose acetate membranes, (**C**, **D**) *ex-vivo* profiles and drug retention (after 24 h) via dorsal skin; "G3": F18 in HEC gel, "G12": F4 (nano without lipid) in HEC gel, "reference": marketed drug, "G10": SSD solution in 1.5% HEC gel, "G11": SSD suspension in HEC gel

Table 6 Stability characterizations of SSD nanocrystal-based hydrogel G3 over 1 week to 4 weeks of storage (mean ± SD, $n = 3$) (30 °C. 75%)

Time	Visual appearance	pH	Theoretical SSD content (%)
Initial time	+++	6.34	109.74 ± 0.49
After 1 week	+++	6.31	106.65 ± 0.85
After 2 weeks	+++	6.35	108.24 ± 0.39
After 3 weeks	+++	6.32	108.74 ± 0.87
After 4 weeks	+++	6.29	105.14 ± 0.77

+++ Completed visual appearance (white, smooth, and homogeneous state)

Meanwhile, Fig. 4B showed that wet-milled nanoparticles (F4 and F18) significantly improved permeability of the drugs compared to SSD raw suspension (in which SSD was milled by pestle and mortar). Interestingly, while cellulose acetate is a hydrophilic substance, F18 (with GMS and lecithin) exhibited a better permeability profile compared with F4. It can be said that the lipid ingredients should have some effects as a diffusion enhancer or lipid ingredient did cover surface of SSD to produce a better permeability.

Drug Release and Retention in Ex-vivo Skin Studies

Figure 4 (C and D) shows the drug release in *ex-vivo* study. This result was correlating to Fig. 4B (in vitro drug release via cellulose acetate membrane). The result can be explained by skin physiology, SSD lipid and water insolubility, particle size and SSD nanostructure. The corneum, epidermis layers contain tight junction of epidermal cell matrix are like Cellulose-acetate membrane in the *in-vitro* test. Thus, the ability of raw SSD (at the micro-scale) to permeate was limited, whereas the permeation rate of SSD nanoparticles was higher. However, compared to cellulose-acetate membrane, the adjacent-cell area contained lipid bilayer which suppressed the permeation of both lipophilic and hydrophilic substance [25], which prevents the penetration of water-insoluble-drug loaded lipophilic nanoparticles. Figure 4B showed that the *ex-vivo* permeation of SSD loaded-lipid nanoparticle was in a slower rate than in *in-vitro* experiment (Fig. 4B). In which, SSD nanoparticles were supposed to be in fatty layers and accumulated in the outer epithelial junctions of the skin (right above the subcutaneous layers). Again, when compared G12 (F4 nanosuspension without lipid ingredients) and G3 (F18), the lipid ingredients did enhance the permeation of drug via the skin. In Fig. 4D, the drug retained in the skin was in a similar trend to the permeation study.

Characterization and Stability of the Chosen Hydrogel

Characteristics including visual appearance, pH, and theoretical drug content of the chosen SSD nanocrystal-based hydrogel were shown in Table 6. The chosen SSD nanocrystal-based hydrogel was stable with no observable change in physical properties in 4 weeks of storage under a temperature of 30 °C and relative humidity of 75% (Table 6). However, there was a reducing trend in term SSD content (from 109 to 105%).

Surface Morphology of the chosen SSD nanocrystal-based hydrogel containing 1.5% HEC was shown in Fig. 5. These SEM images determined that HEC played an important role in forming a homogeneous and stable network containing SSD nanocrystal particles. The particle sizes of SSD crystals were about 300 nm, which was appropriate to SSD nanocrystal particle sizes measured by a dynamic light scattering analyzer (Zetasizer Ultra Nano ZS90).

SSD nanoparticles, composed in lipid matrix of GMS (discussed in 3.1.5), were dispersed in the gel matrix. In which, (i) the hydrophilic ingredients (PVA or HPMC) and also (ii) the mobility of nanoparticles facilitated the SSD nanoparticle dispersion into the hydrogel. In return, the lipid-SSD NPs were trapped inside hydrogel matrix, preventing them from aggregation and enhancing its stability

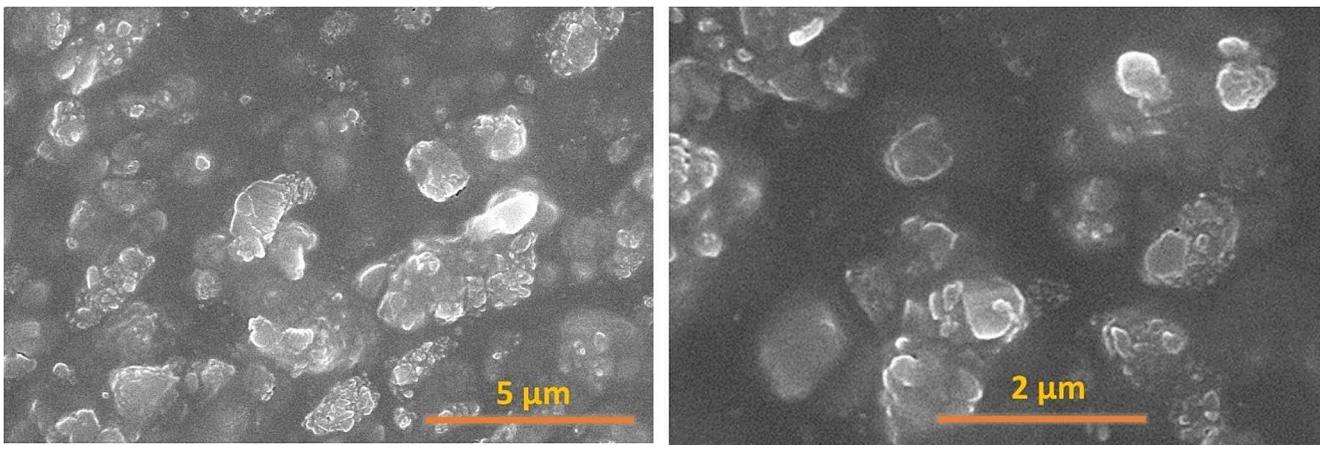

Fig. 5 Representative SEM images of hydrogel G3 (F18 in HEC gel)

[26, 27]. From pharmaceutical quality, together with the stability data in 4 weeks (3.1.4), the formed SSD nanoparticles should be prepared in the gelling agent as soon as possible.

In vitro Antimicrobial Activity Studies

Minimum Inhibition Concentration (MIC) and Zone of Inhibition

SSD nanocrystal-based hydrogel showed in vitro antimicrobial activity on *Staphylococcus aureus (S.aureus)* and *Escherichia coli (E.coli)*. The results showed that SSD and SSD-nanoparticle exhibited a similar MIC values (at 16 and 32 µg/mL, respectively for *E.coli and S.aureus*). This result is consistent with previous study about SSD, which was effective in targeting these bacteria [3, 13, 14].

Effects of different samples were also shown via the zone of inhibition (disk diffusion experiment on *S. aureus* and *E.coli* cultures). Regarding *S.aureus*, SSD nanoparticle gel (2.35 ± 0.05 mm) and SSD raw-suspension (2.11 ± 0.01 mm) showed a significantly higher effect compared to solution (1.80 ± 0.02 mm) and market reference (1.38 ± 0.04 mm, Fig. 6A). A similar trend was obtained with *E.coli*: SSD nanoparticle gel (1.76 ± 0.04 mm) and SSD raw-suspension (2.02 ± 0.07 mm), while the diameter of the inhibition zone were 0.6 ± 0.01 mm (reference gel) and 0.6 ± 0.01 mm (solution gel) (Fig. 6A). Thus, the finding showed that when preparing SSD in the form of suspension (raw or nanoparticle), the permeability and diffusion via agar gel were higher than molecular formulation (solution gel or marketed reference).

Biofilm (Staphylococcus aureus) Experiments

Based on biofilm results as shown in Fig. 6B, SSD solution and SSD nanoparticles exhibited a dose-dependent CFU-suppression effect. Solution samples and SSD nanoparticles exhibited CFU-suppression values at concentrations of 128 and 256 µg/mL. At lower concentration (for example: 64 µg/

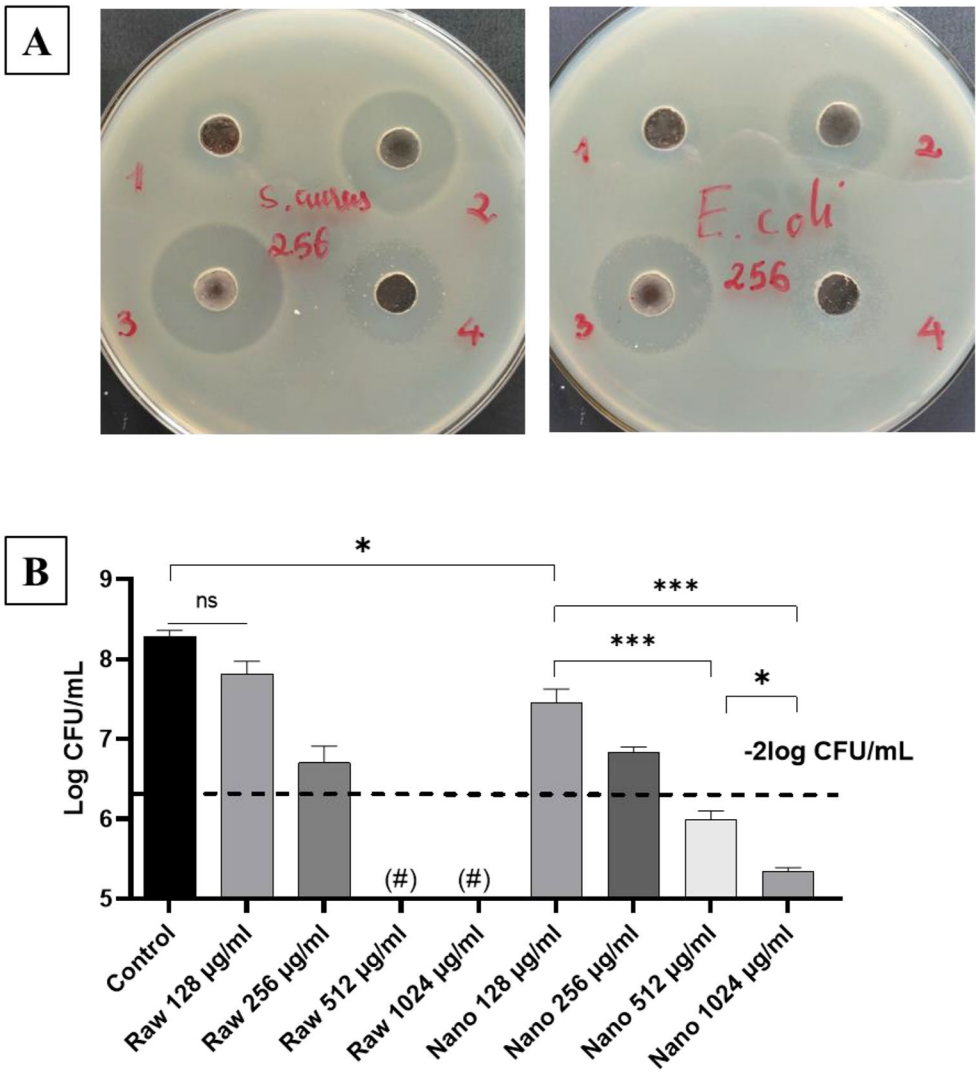

Fig. 6 (**A**) disc-diffusion antibiotic susceptibility test on *S. aureus* (left) and *E.coli* (right): (1) SSD solution, (2) SSD nanohydrogel, (3) SSD suspension, (4) Reference; (**B**) Dose-dependent effect of SSD and SSD-nanoparticle on biofilm: 128 to 1024 µg/ml, (#) SSD-raw at 512 and 1024 µg/mL were precipitated. (*): $p < 0.05$, ***: $p < 0.001$ (Silver sulfadiazine nanocrystal-based hydrogels: The impact of lipid components on *in-vitro* and *ex-vivo* release, bacterial biofilm permeability, and *in-vitro* antibacterial activity)

mL), all samples showed no significant effect (-LogCFU was -0.03 ± 0.085). Compared to MIC values (32 µg/mL on *S.aureus*), in the biofilm experiment, the SSD concentration required to show CFU-suppression effect was higher (from 256 µg/mL); that was probably due to the effect of biofilm [28]. Interestingly, while there was not statistically difference between control and SSD solution at 128 µg/mL, there was a statistically difference between control and SSD nanoparticles ($p < 0.05$). The stronger biofilm-effect of nanoparticles was probably caused by the increasing permeation and diffusion of nanoparticles via biofilm membrane. At concentration of 256 µg/mL, the effect of nanoparticles was subdued by the dose-effect of SSD (there was no significant difference between SSD solution and SSD nanoparticle). At higher concentrations (512 and 1024 µg/mL), SSD nanoparticles displayed significant effects, in which the CFU-suppressions were less than 1/100 of the control sample ($p < 0.05$). The delta log CFU/mL of SSD-nanoparticles (512 and 1024 µg/mL) were -2.29 and -2.94, respectively. On the other hand, at 512 and 1024 µg/mL concentrations, SSD in the solution sample were precipitated due to low solubility, as the experiment was not able to continue and validified. In contrast, SSD nanoparticles were suspended and dispersed homogeneously in the 96-well to exhibit a dose-dependent antibacterial effect. In sum, preparing SSD nanoparticles did improve antibacterial effect on biofilm experiments.

About the biofilm experiment, this model was established and validated to screen the effect of antibiotics as well as different antibacterial agents [17, 29]. Here, *in-vitro* biofilm requires a higher concentration of SSD to suppress bacterial growth. That result was complied with previous publications as biofilm did limit drug-efficacy on bacteria [9, 10]. In terms of the *in-vivo* experiment and clinical trials, higher drug concentrations at the target site can be achieved by using (i) a higher dose at the site of infection or (ii) an increasing frequence of treatments. As mentioned, SSD nanoparticles offered an effective way to increase both permeability and higher concentrations of SSD at the target site. Particularly, in the *in-vitro* biofilm test, SSD solution or raw-suspension were unable to prevent SSD precipitation at the same concentration, 512–1024 µg/mL. Aiming for *in-vivo* experiment in future, our study offered an approach for improving therapeutic efficacy and safety; future clinical indications should be based on the extent of the burn injury, the thickness of the burn, and the patient's age and weight.

Biofilms are composed of a complex matrix called extracellular polymeric substances (EPS), which include both hydrophilic and hydrophobic components [28]. Hydrophilic components are polysaccharides, proteins, and extracellular DNA in the EPS matrix, while lipids and lipoproteins, hydrophobic ingredients, contribute to the stability of the biofilm structure [28, 30]. Hereby, the first nanoparticles of drug can be designed to be such a small size that allows them to penetrate the pores and crevices of the EPS matrix. In this case, the second lipid components of G3 formulation enhance their interaction with the biofilm's components, potentially facilitating penetration. Then, silver ions in SSD nanoparticles can interact to the negatively charged polysaccharides in the EPS matrix, leading to the disruption of the matrix's structural integrity [30, 31]. Silver ions have been reported to interfere with quorum sensing, which can lead to disruptions in biofilm development and the expression of virulence factors [30, 32]. Interestingly, both silver and sulfonamides have been reported to affect quorum sensing, the communication mechanism used by bacteria in biofilms to coordinate their behavior. Disrupting quorum sensing can interfere with biofilm development and the expression of virulence factors. However, silver ions and sulfadiazine's effectiveness was limited by their ability to penetrate the biofilm and reach the bacterial cells [31]. The concentration and exposure time of sulfadiazine are important factors in term of both antibacterial effects and antibiotic-resistance [31, 33]. In this case, preparation of SSD nanoparticles is a suggestion for clinical application. As discussion, SSD nanoparticles increased permeation of SSD into the hydrophilic layers (like CA membranes), which are suitable for biofilm treatment. Additionally, SSD nanoparticle-loaded hydrogel only released and retained drug in the epithelial layers of the skin, which is important to maintain a dose regime and time-of treatment.

Conclusions

In this our research, SSD nanocrystal-lipid carrier-based hydrogels were developed for enhanced dermal drug retaining and in vitro antimicrobial activity. The combination of lipid ingredients in SSD nanoparticle preparation (wet-milling technology) was proved (via artificial neural networks) in terms of physicochemical properties and stability of nanosuspension, dermal drug retaining and antibacterial activity in the biofilm model. This finding implied a potential application of nanocrystal-lipid carrier-based hydrogels for future pharmaceutical innovation.

Acknowledgements This research did not receive any specific grant from funding agencies in the public, commercial, or not-for-profit sectors.

Funding Not applicable.

Declarations

Conflict of interest The authors declare no conflict of interest.

Ethical Approval Not applicable.

References

1. Eming SA, Krieg T, Davidson JM. Inflammation in wound repair: molecular and cellular mechanisms. J Invest Dermatology. 2007;127(3):514–25.
2. Miller AC, Rashid RM, Falzon L, Elamin EM, Zehtabchi S. Silver sulfadiazine for the treatment of partial-thickness burns and venous stasis ulcers. J Am Acad Dermatol. 2012;66(5):e159–65.
3. Hoffmann S. Silver sulfadiazine: an antibacterial agent for topical use in burns. Scand J Plast Reconstr Surg. 1984;18(1):119–26.
4. Ueda Y, Miyazaki M, Mashima K, Takagi S, Hara S, Kamimura H et al. The effects of silver sulfadiazine on methicillin-resistant Staphylococcus aureus biofilms. 2020;8(10):1551.
5. Kumar PM, Ghosh A. Development and evaluation of silver sulfadiazine loaded microsponge based gel for partial thickness (second degree) burn wounds. Eur J Pharm Sci. 2017;96:243–54.
6. Naser NA, Alasedi KM, Khan ZA. New approach for determination of sulfadiazine in pharmaceutical preparations using 4 (4-sulphophenylazo) pyrogallol: kinetic spectrophotometric method. Spectrochim Acta Part A Mol Biomol Spectrosc. 2018;201:267–80.
7. Nesbitt RU Jr., Sandmann BJ. Solubility studies of silver sulfadiazine. J Pharm Sci. 1977;66(4):519–22.
8. Pharmacopoeia J. Japanese Pharmacopoeia 17: Official Monographs Sulfadiazine Silve. 2016.
9. Costerton JW, Stewart PS, Greenberg EPJ. Bacterial biofilms: a common cause of persistent infections. 1999;284(5418):1318–22.
10. Jahangir MA, Imam SS, Muheem A, Chettupalli A, Al-Abbasi FA, Nadeem MS, et al. Nanocrystals: characterization overview, applications in drug delivery, and their toxicity concerns. J Pharm Innov. 2022;17(1):237–48.
11. Venkataraman M, Nagarsenker M. Silver sulfadiazine nanosystems for burn therapy. AAPS PharmSciTech. 2013;14(1):254–64.
12. Gao L, Gan H, Meng Z, Gu R, Wu Z, Zhu X, et al. Evaluation of genipin-crosslinked chitosan hydrogels as a potential carrier for silver sulfadiazine nanocrystals. Colloid Surf B: Biointerfaces. 2016;148:343–53.
13. Liu X, Gan H, Hu C, Sun W, Zhu X, Meng Z et al. Silver sulfadiazine nanosuspension-loaded thermosensitive hydrogel as a topical antibacterial agent. Int J Nanomed. 2019:289–300.
14. Mastiholimath VS, Valerie CTW, Shrishailappa V, Mannur PMD, Gadad AP, Khanal P. Formulation and evaluation of solid lipid nanoparticle containing silver sulfadiazine for second and third degree burn wounds and its suitable analytical method development and validation. Indian J Pharm Educ Res. 2020;54:31–45.
15. Malamatari M, Taylor KM, Malamataris S, Douroumis D, Kachrimanis K. Pharmaceutical nanocrystals: production by wet milling and applications. Drug Discovery Today. 2018;23(3):534–47.
16. Peltonen L, Hirvonen J. Pharmaceutical nanocrystals by nanomilling: critical process parameters, particle fracturing and stabilization methods. J Pharm Pharmacol. 2010;62(11):1569–79.
17. Nguyen TK, Peyrusson F, Siala W, Pham NH, Nguyen HA, Tulkens PM, et al. Activity of Moxifloxacin Against Biofilms formed by clinical isolates of Staphylococcus aureus Differing by their resistant or Persister Character to fluoroquinolones. Front Microbiol. 2021;12:785573.
18. Tuomela A, Hirvonen J, Peltonen LJP. Stabilizing agents for drug nanocrystals: effect on bioavailability. 2016;8(2):16.
19. Sargam Y, Wang K, Tsyrenova A, Liu F, Jiang S. Effects of anionic and nonionic surfactants on the dispersion and stability of nanoSiO2 in aqueous and cement pore solutions. Cem Concr Res. 2021;144:106417.
20. Attama AA, Momoh MA, Builders PF. Lipid nanoparticulate drug delivery systems: a revolution in dosage form design and development. Recent Adv Novel drug Carrier Syst. 2012;5:107–40.
21. Tran BN, Tran HT, Le GT, Tran HP, Le KN, Do HH et al. Solidifying Fenofibrate Nanocrystal Suspension: A Scalable Approach via Granulation Method. 2023;2023.
22. Tran BN, Nguyen HT, Kim JO, Yong CS, Nguyen, CNJAopr. Combination of a chemopreventive agent and paclitaxel in CD44-targeted hybrid nanoparticles for breast cancer treatment. 2017;40:1420–32.
23. Bult A, Plug CM. Silver sulfadiazine. Analytical profiles of Drug Substances. Volume 13. Elsevier; 1984. pp. 553–71.
24. Sheskey PJHB, Moss GP, Goldfarb DJ. Handbook of pharmaceutical excipients: Edition 9. Pharmaceutical; 2020.
25. Iwai I, Han H, Hollander Ld, Svensson S, Öfverstedt L-G, Anwar J, et al. The human skin barrier is Organized as stacked bilayers of fully extended ceramides with Cholesterol Molecules Associated with the Ceramide Sphingoid Moiety. J Invest Dermatology. 2012;132(9):2215–25.
26. Dannert C, Stokke BT, Dias RS. Nanoparticle-hydrogel composites: from molecular interactions to macroscopic behavior. 2019;11(2):275.
27. Tran BN, Tran KL, Nguyen TT, Bui LT, Nguyen CN. A Novel Alginate Film based on Nanocoating Approach for enteric-release tablets. AAPS PharmSciTech. 2023;24(4):99.
28. Nguyen TK, Argudín MA, Deplano A, Nhung PH, Nguyen HA, Tulkens PM et al. Antibiotic resistance, biofilm formation, and intracellular survival as possible determinants of persistent or recurrent infections by staphylococcus aureus in a Vietnamese tertiary hospital: focus on bacterial response to moxifloxacin. 2020;26(6):537–44.
29. Siala W, Kucharíková S, Braem A, Vleugels J, Tulkens PM, Mingeot-Leclercq M-P, et al. The antifungal caspofungin increases fluoroquinolone activity against Staphylococcus aureus biofilms by inhibiting N-acetylglucosamine transferase. Nat Commun. 2016;7(1):13286.
30. Cerca N, Pier GB, Vilanova M, Oliveira R, Azeredo, JJRim. Quantitative analysis of adhesion and biofilm formation on hydrophilic and hydrophobic surfaces of clinical isolates of Staphylococcus epidermidis. 2005;156(4):506–14.
31. Mizdal CR, Stefanello ST, da Costa Flores V, Agertt VA, Bonez PC, Rossi GG et al. The antibacterial and anti-biofilm activity of gold-complexed sulfonamides against methicillin-resistant Staphylococcus aureus. 2018;123:440–8.
32. Vaze N, Demokritou P. Using engineered water nanostructures (EWNS) for wound disinfection: case study of Acinetobacter baumannii inactivation on skin and the inhibition of biofilm formation. Nanomed Nanotechnol Biol Med. 2022;42:102537.
33. Siqueira FS, Alves CFS, Machado AK, Siqueira JD, Santos Td, Mizdal CR et al. Molecular docking, quorum quenching effect, antibiofilm activity and safety profile of silver-complexed sulfonamide on Pseudomonas aeruginosa. 2021;37(5):555–71.